ENVIRONMENTAL MONITORING OF DUST STORMS OVER THE NILE DELTA, EGYPT USING MODIS SATELLITE DATA

Hesham EL-ASKARY[1], Menas KAFATOS[1] & Mohamed HEGAZY[2]

[1]CEOSR/School of Computational Sciences
George Mason University Fairfax, VA, USA
[2]National Authority for Remote Sensing and Space Sciences, Cairo, Egypt
helaskar@scs.gmu.edu, mkafatos@gmu.edu, mhegazy1@gmu.edu

ABSTRACT

Egypt is located within the arid and semi arid northeastern Africa. Part of it is within the Northern African Sahara. Air pollution from dust storms is considered as a serious problem in several Egyptian cities. Blown sand and dust originating in the Western Desert create an almost permanent haze over big cities, such as Cairo and Alexandria. The present work studies the dust storms over the Nile Delta, and searches for their cause, extension and time of occurrence. We use the MODIS sensor to provide remote sensing data.

1 INTRODUCTION

The aim of this study is to identify features related to dust storms, encountered in the Nile Delta region. The study is based on remote sensing and attempts to interpret certain features found in the Western part of the Delta only. Although the features have the appearance of clouds, their absence over the eastern part of the delta is hard to explain. Moreover, according to existing data (Meteorological Atlas of Egypt 1996), the wind prevailing during September is coming from south to southwest directions.

Based on the analysis presented here and data processing, the dust storms over the western part of the Nile Delta can be monitored using MODIS data and the overall environmental issues for these features could be further clarified.

2 THE USED SATELLITE DATA SETS

The data used in this study are obtained from the MODIS (Moderate Resolution Imaging Spectroradiometer) sensor onboard the *Terra* EOS platform. This sensor is characterized by wide spectral range, having 36 channels, and moderate spatial resolution that ranges from 250 m to 1km. MODIS was found to be suitable for monitoring environmental changes (Kafatos et al 2000) in Egypt.

Two MODIS L-1B 1-km data sets over Egypt obtained on September 1st 2000 and September 3rd 2000 have been used. The level 1B products don't directly contain images but they contain the calibrated data for other software applications to construct the images.

The format of the acquired raw data sets is the widely used Hierarchical Data Format-Earth Observing System (HDF-EOS). Along with these HDF files, other HDF.met files were obtained. These are the metadata files containing information about the used data set as well as the location and the time of acquisition.

The reflectances obtained from the L1B data sets for the two dates are displayed (Figures 1 and 2). (Figures 3 and 4) are higher-level products contained in the HDF file, and represent aerosol index. The two figures are used in our analysis whereas the colored insert areas in both figures represent the regions of interest.

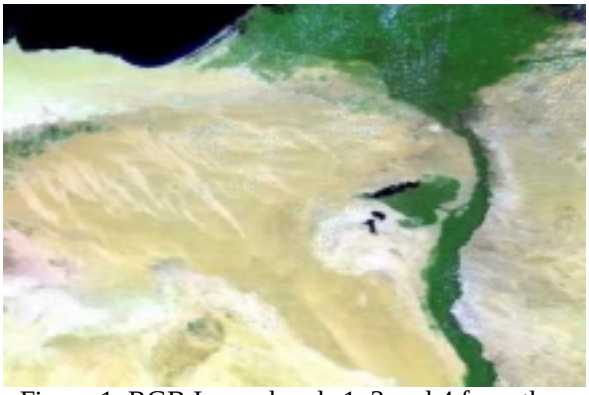

Figure 1. RGB Image bands 1, 3 and 4 from the L1B original Data set on the September 1st 2000

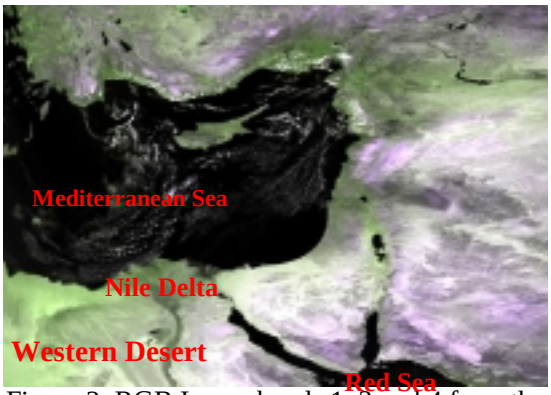

Figure 2. RGB Image bands 1, 3 and 4 from the L1B original Data set on the September 3rd 2000

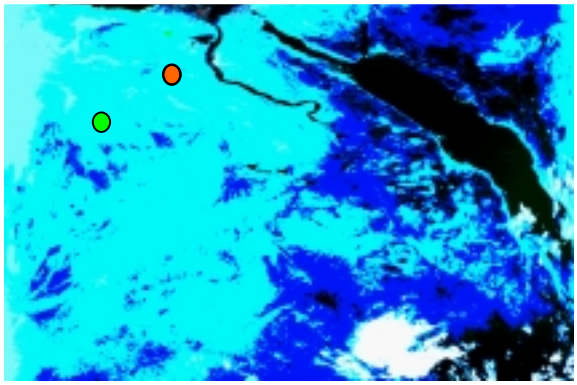

Figure 3. RGB Bands 1, 3 and 4 Earth view reflectance solar bands uncertainty index (Aerosol Index), September 1st.

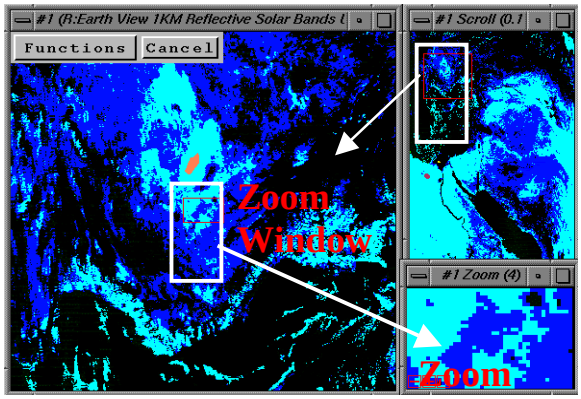

Figure 4. RGB Bands 1, 3 and 4 Earth view reflectance solar bands uncertainty index (Aerosol Index), September 3rd.

Table 1. Electromagnetic spectral regions of interest.

Region	Color	Description
Region # 1	Red	Observed features in the Delta September 1st 2000
Region # 2	Green	The western desert for both September 1st and 3rd 2000
Region # 3	Orange	Turkey located north of Egypt.
Region # 4	Yellow	Clear Delta with no features shown in the scroll window for September 3rd 2000

3 INTRODUCTION TO THE USED SOFTWARE (ENVI)

The ENVI software (Environment for Visualizing Images) is suitable for MODIS data sets, since it can handle a lot of different data formats like HDF-EOS. It allows the user to perform transformations, classifications (supervised and unsupervised), as well as spectral unmixing and filtering using end members from the image itself or from the spectral libraries, and N-D visualizer for viewing the data dynamically.

In this work, ENVI is used for unsupervised classification, extracting spectral signatures of the pixels from the regions of interest for their comparison, as well as doing Principal Component Analysis for noise removal.

4 IMAGE CLASSIFICATION

The main objective of this operation is to identify different features in the scene by replacing the visual analysis of the image data with quantitative information in order to determine the land cover identity of each pixel in an image, and to categorize all pixels in an image into land cover classes or

themes. Classification is divided into supervised and unsupervised and the choice of one of these two techniques depends upon the aim of the study. In the present work we believe that the unsupervised technique will be better because we are looking for the identification of some general features. The specific class they belong to is important, although we are not attempting to identify specific materials for which we would need supervised classification and spectral libraries. Another important reason for using unsupervised classification is the lack of ground truth information.

4.1 UNSUPERVISED CLASSIFICATION

Unsupervised classification is a method, which examines a large number of unknown pixels and divides them into a number of classes based on natural groupings present in the image values. The resultant classes are spectral classes, whose identity is initially unknown. They must be compared with some forms of reference data (from larger scale imagery, maps or site visits) to determine their identity and informational values. (Lillesand and Kiefer, 1994).
Unsupervised classification using statistics only is an analytical procedure based upon clustering by using different algorithms; some of them will be discussed later; they can be used for the classification of any image in our case to obtain an idea about the discovered strange features to identify to which class they belong. K-Means and Isodata are two different unsupervised classification techniques, which have been used, in the present work.

4.1.1 K-MEANS ALGORITHMS

The K-means algorithm uses both the spatial and the spectral properties of the multispectral image for clustering, and produces a partition of a discrete set of objects into a smaller discrete set of classes. A good clustering result is when the objects in the same class are more or less alike, and objects in different classes are in some sense different (Lillesand and Kiefer, 1994). The algorithm arbitrarily selects seed or start positions for the "K" clusters. Each pixel of the image data is then assigned to the cluster whose mean vector is closest to the pixel vector. A new set of mean vectors for a particular class is then calculated from the results of the previous classification and the pixels are reassigned to the new cluster vectors. The procedure continues until there is no significant change in pixel assignments from one iteration to the next, or when the iterations have reached the maximum number specified. This technique calculates initial class means evenly distributed in the data space and then clusters the pixels into the nearest class using a minimum distance technique. The pixel classification continues until the number of pixels in each class changes by less than the selected pixel change threshold or the maximum number of iterations is reached.

This technique was carried and applied twice, with the same settings as number of classes = 5, change of threshold = 5% and maximum iterations = 20 once to the September 1st 2000 image (Figure 5), showing how these unknown features tend to be similar to the same class as the desert class for both the Western and Eastern parts of Egypt. The second time was for the September 3rd 2000 image, (Figure 6), which shows how much the Nile Delta is free from any features, as well as having similar features in Turkey that tend to be in the same class as the deserts.

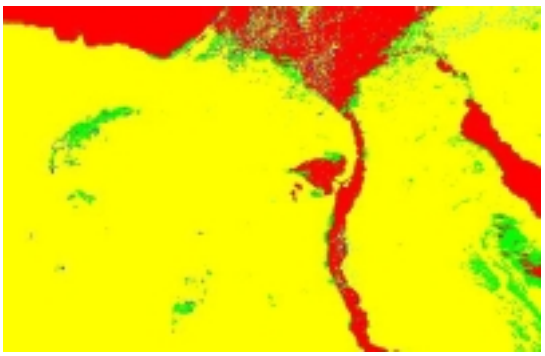

Figure 5. Unsupervised classified image using the K-means algorithm applied on data set obtained on September 1st 2000.

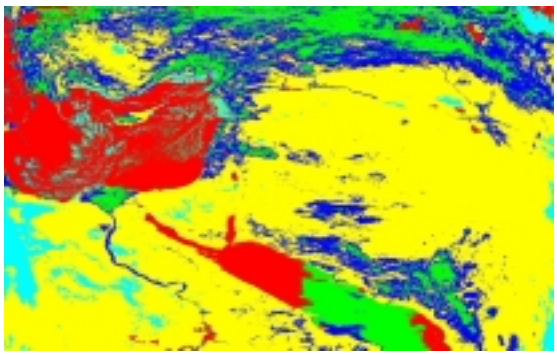

Figure 6. Unsupervised classified image using the K-means algorithm applied on data set obtained on September 3rd 2000.

4.1.2 ISODATA

The Isodata algorithm is basically an extension of the K-Means algorithm. The user specifies the number of desired clusters and optionally specifies the initial set of cluster mean vectors. Unlike K-Means, however, after each iteration, Isodata statistically examines each cluster and applies cluster splitting, merging, or discarding according to some defined criteria. This may lead to the resultant category number not to agree with the number initially specified. In this study, when using three bands (band1, band3 and band4) with 5 categories (5 classes) and 20 iterations specification, Isodata usually produced almost identical result as the K-Means, (Jia and Richards, 1993). This technique is based upon estimating some reasonable assignment of the pixel vectors into candidate clusters and then moving them from one cluster to another so that the sum of squared error (SSE) measure of the preceding class is reduced. This process continues until the number of pixels in each class changes by less than the selected pixel change threshold or the maximum number of iterations is reached. The specified settings were number of classes = 5(min), 10(max); maximum iterations = 20, change threshold = 5%, min number of pixel in class = 0, max class Stdv = 1 and min class distance = 5. The images of September 1st (Figure 7) and September 3rd (Figure 8) are presented here.

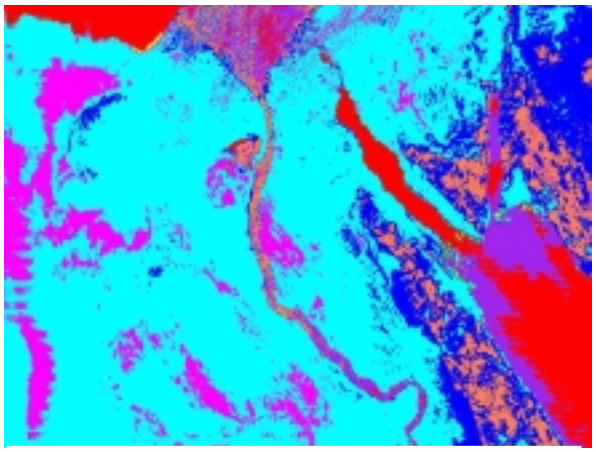

Figure 7. Unsupervised classified image using the Isodata algorithm, applied on data set obtained on September 1st 2000.

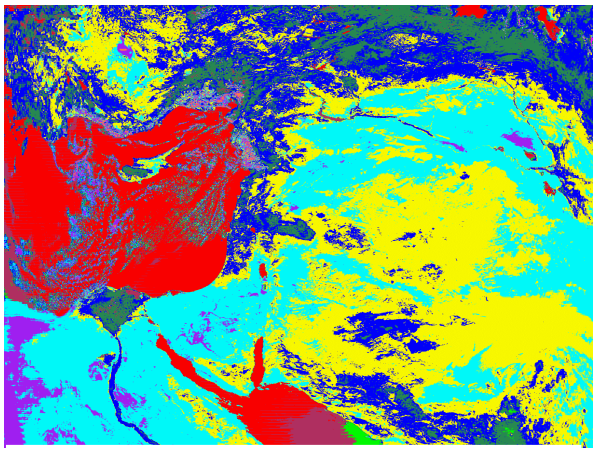

Figure 8. Unsupervised classified image using the Isodata algorithm, applied on data set obtained on September 3rd 2000.

5 Z-PROFILE

We have determined an on-the-fly spectral average of selected pixels. This spectral average is plotted in the Spectral Profile window, and it has been used to determine the spectral signatures of different pixels in the areas under study. Using this function it was easy to compare the spectral signatures of pixels from the unknown features in the Nile Delta with others from the Western Desert as well as with other pixels located in Turkey (Chavez, 1988).

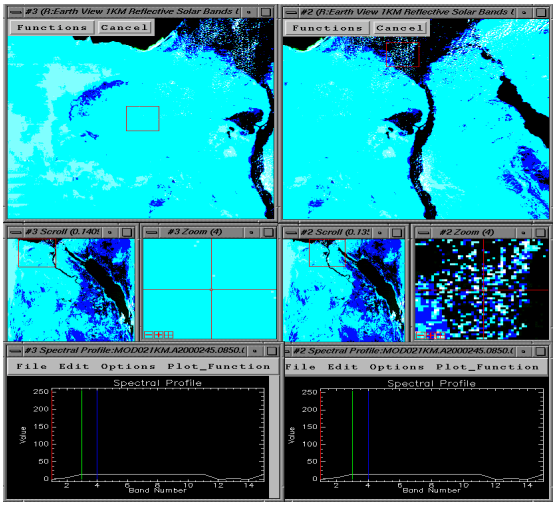

Figure 9. Matching of the spectral signatures for some pixels from the features in the Nile Delta and from the Western Desert on September 1st 2000.

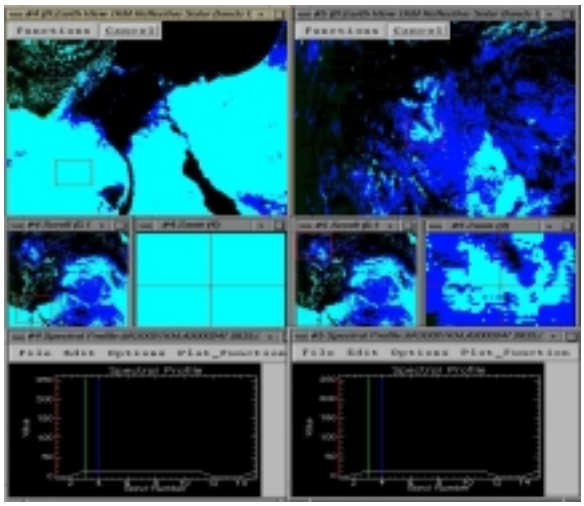

Figure 10. Matching of the spectral signatures for some pixels from Turkey and from the Western Desert in Egypt on September 3rd 2000.

By making this comparison on the original data sets after applying the classification algorithms, the obtained results were promising in the sense that spectral signatures for the selected pixels were similar to others from different locations. The results of this analysis are shown in (Figures 9 and 10) for September 1st and September 3rd, respectively, corresponding to September 1st 2000 and September 3rd 2000 data.

6 PRINCIPAL COMPONENT ANALYSIS

Principal Components Analysis (PCA), often referred to as a PC rotation, is a linear transformation of a multivariate dataset into a new coordinate system. For remote sensing applications, the multiple variables are typically the different wavelengths of a multispectral or hyperspectral image cube.

Principal and canonical component analysis in general increases the computational efficiency of the classification process because it may reduce the dimensionality of the original data set. These transformations may be applied either as an enhancement operation prior to visual interpretation of the data or as a preprocessing procedure prior to automated classification of the data.

It generates a new set of variables, which are used to describe multispectral remote sensing data. These new variables, or principal components, are such that the first few contain most of the variance in the original data. Moreover, in these principal component axes, the data are uncorrelated. Owing to this it has been used as a data transform to enhance regions of localized change in multitemporal and multispectral image data. This is a direct result of the high correlation that exists between image data for regions that do not change significantly and the relatively low correlation associated with regions that change substantially. Provided the major portion of the variance in a mutlitemporal image data set is associated with constant cover types, regions of localized change will be enhanced in the higher components of the set of images generated by a principal components transformation of the multitemporal, multispectral data. The principal component analysis is applied until maximizing the variance of the data.

The covariance matrix is a square, symmetric matrix of size [bands x bands] where the diagonal elements are band variances and the off-diagonals are band covariances. The correlation matrix is equivalent to a covariance matrix for an image where each band has been standardized to zero mean and unit variance. This method tends to equalize the influence of each band, inflating the influence of bands with relatively small variance and reducing the influence of bands with high variance. While it is less common to use this approach for normal remote sensing datasets, there are special situations

when this method is preferable. The eigen vectors and the eigen values of the covariance matrix and the number of the PC components obtained from the original data set determine the results of this analysis. In this case 15 PC components were obtained from 15 bands for each data set at the two different times.

The obtained results were satisfactory as for the September 1st 2000 dataset the first four principal components contain more than 90% of the total variance (PC1 54.3%, PC2 20.5%, PC3 8.3% and PC4 7.4%). For the September 3rd dataset the first four principal components contain more than 90% of the total variance (PC1 62.2%, PC2 19.8%, PC3 7.7% and PC4 4.1%). The gray scale images obtained from the first PC components are shown in (Figures 13 and 14) for the two different time periods, respectively.

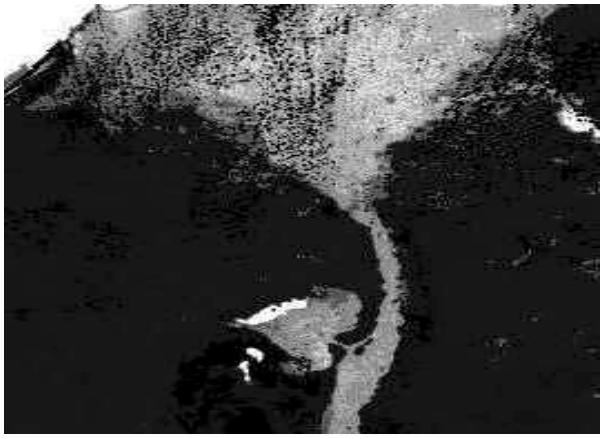

Figure 13. Gray scale image of PC1 for the September1st 2000 dataset.

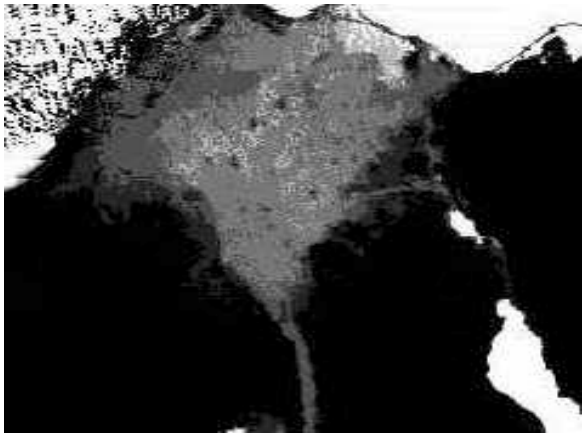

Figure 14. Gray scale image of PC1 for the September3rd 2000 dataset

These figures contain a lot of information about these features as in the September 1st, the features are strong, and in the September 3rd, there are almost no features present. This result confirms identification of these features, namely that they are fine dust coming from the Western Desert in the form of dust storm and then moving to other locations to the north of Egypt. Although the comparison between the two PCs is not totally adequate because there are different features contributing the formation of these PCs in the two different time periods, yet it is very obvious that there is a big difference in the Delta region in the two images. Future work will carry out accurate georegisteration of different images taken at different times to identify features contributing in the formation of the PCs for much more finalized results.

Two RGB images were created using the first three PCs from the September 1st and September 3rd data sets (Figures 15 and 16).

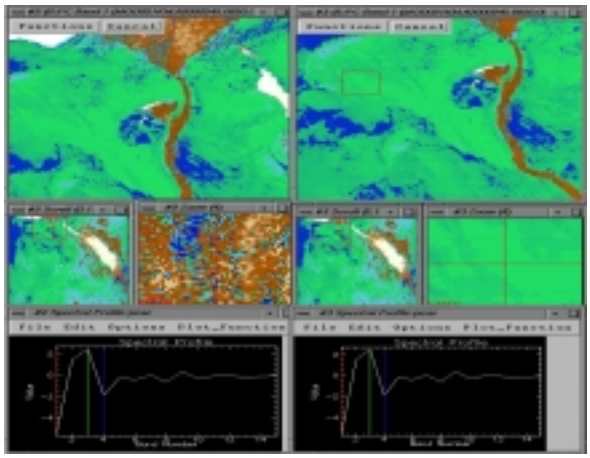

Figure 15. RGB image of the PC1, PC2 and PC3 from the September 1st dataset.

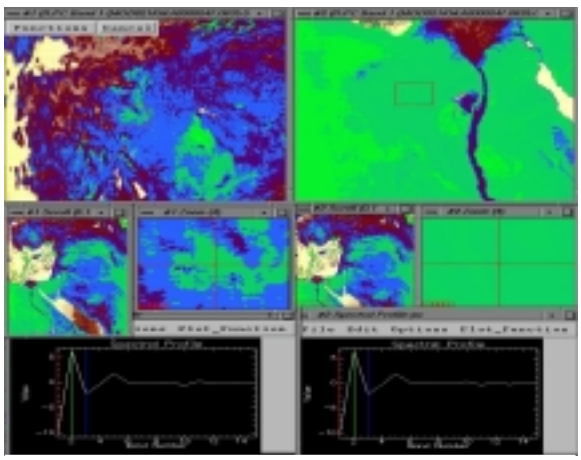

Figure16. RGB image of the PC1, PC2 and PC3 from the September 3rd dataset.

The results were much more obvious and the Z-profile obtained from the some pixels in the Delta and the Western Desert was matching very well after the noise removal using PCA. The Z-profile obtained from pixels in the Western Desert and in Turkey from the second data set showed that the signatures were matching very well.

7 CONCLUSIONS

• The MODIS sensor can be used to detect dust storms and the data can provide information on the direction of wind causing these storms.
• The wind causing the straight alignment behavior of the fine dust over the Nile Delta appears to be blowing from the south to the north otherwise they would be scattered over the entire Delta region and not only in some part of it.
•There might be a difference in the physical properties between the sand found in the Western Desert and that from the East, rather than in their chemical properties, as the reflectances coming from both are exactly the same. The concentration of dust in the western part of the Delta and not in the entire Delta region showed that the Eastern Desert sand is much coarser than that coming from the Western Desert. As a result, the south winds didn't succeed in transporting sands from the Eastern desert. It can be also due to the rocky surfaces prevailing there and the rare occurrence of sand dunes and sheets.

REFERENCES

Chavez, Pat S. Jr., 1988. An Improved Dark-Object Subtraction Technique for Atmospheric Scattering Correction of Multispectral Data. Remote Sensing of Environment. 24:459-479.

Egyptian Meteorological Authority, 1996. Climatic Atlas of Egypt. 157. Cairo.

ENVI 3.2, Environment for Visualizing Images Tutorial 4.

Jackson J. E, 1991. A user's guide to Principal Component Analysis.

Jia, X. and Richards, J. A., 1993. Binary coding of imaging spectrometer data for fast spectral matching and classification". Remote Sensing of Environment, 43, 47-53.

Kafatos, M. et.al., 2000. The Moderate Resolution Imaging Spectroradiometer (MODIS): Potential Remote Sensing Applications of Natural Resource and Environment Monitoring in Egypt

Lillesand, T. M., and R. W. Kiefer, 1994. Remote Sensing and Image Interpretation. 3rd Edition, John Wiley and Sons, New York.

Sabins, F.F., 1978. Remote Sensing principles and interpretation, San Francisco: Freeman, 524 p.4.